

Magnetic properties of the two allotropic phases of PuGa₃

P. Boulet,¹ E. Colineau,¹ F. Wastin,¹ P. Javorský,^{1,2} J. C. Griveau,¹ J. Rebizant,¹ G. R. Stewart,³ and E. D. Bauer⁴

¹European Commission, Joint Research Centre, Institute for Transuranium Elements, P.O. Box 2340, 76125 Karlsruhe, Germany

²Faculty of Mathematics and Physics, Department of Electronic Structures, Charles University, Ke Karlovu 5, 12116 Prague 2, The Czech Republic

³Department of Physics, University of Florida, Gainesville, Florida 32611, USA

⁴Los Alamos National Laboratory, Los Alamos, New Mexico 87545, USA

(Received 30 March 2005; revised manuscript received 21 June 2005; published 19 August 2005)

PuGa₃ crystallizes in either a trigonal structure type ($R\bar{3}m$) or in the hexagonal DO19 type ($P6_3/mmc$). The magnetic properties of both allotropes were investigated by magnetization, specific heat, and electrical resistivity measurements down to low temperatures and under magnetic fields and high pressures. Both phases order magnetically; the trigonal modification corresponds to a soft ferromagnet below $T_c=20$ K with a saturated moment of $0.2 \mu_B/\text{Pu}$, whereas the hexagonal one exhibits antiferromagnetic order below $T_N=24$ K which undergoes a metamagnetic transition at $\mu_0 H_M \approx 6.1$ T (at $T=5$ K). In the paramagnetic state, the effective magnetic moment inferred from a modified Curie-Weiss law amounts to $\mu_{\text{eff}} \approx 0.78 \mu_B$ for both phases, indicative of the occurrence of a Pu³⁺ charge state. The values of the electronic specific heat coefficient $\gamma \approx 110$ and 220 mJ/mol K² for the trigonal and hexagonal allotropes, respectively, indicate a moderate heavy fermion character. Comparisons with related compounds PuCoGa₅, UGa₃, and NpGa₃ suggest a strong tendency toward $5f$ delocalization.

DOI: [10.1103/PhysRevB.72.064438](https://doi.org/10.1103/PhysRevB.72.064438)

PACS number(s): 71.27.+a, 75.30.-m, 74.10.+v

I. INTRODUCTION

The unusual properties of plutonium make it one of the most complex and interesting elements in the periodic table.¹ As illustrated by its six different allotropic phases, plutonium is extremely sensitive to changes in temperature, pressure, or chemistry. As a consequence, its reactivity allows the formation of many compounds, which show interesting chemical and physical properties. Recently, the discovery of superconductivity in the intermetallic compounds PuTGa₅ with $T = \text{Co}$ (Ref. 2) and Rh (Ref. 3) raised a great interest amongst the scientific community. The structural similarities with the unconventional Ce-based compounds CeMIn₅ (Refs. 4 and 5) and the binary pressure-induced superconductor CeIn₃ (Ref. 6) show the importance of the structural parameters. A comparison of the results obtained on the CeCo_{1-x}Rh_xIn₅ and PuCo_{1-x}Rh_xGa₅ (Ref. 7) series, reveals a similar linear variation of T_c versus c/a , with in both cases a $d \ln T_c / d(c/a) \approx 100$, indicating a common underlying physics and highlighting the importance of anisotropy in the occurrence of superconductivity in these structures.

Attention has focused on the rich Pu-Ga binary phase diagram¹ in recent years with regards to the stability of δ -Pu and its possible decomposition into α -Pu and Pu₃Ga. The Pu-Ga phase diagram based on the work of Ellinger *et al.*⁸ or Cheboratev *et al.*,⁹ reveals the existence of 10 intermediate binary compounds. Ellinger *et al.*,⁸ have evidenced a structural phase transition at 922 °C in PuGa₃. The crystal structure of the lower temperature modification was established to be isostructural to the Ni₃Sn structure type, also known in the Strukturbericht designation as DO19. One year later, Larson *et al.*¹⁰ showed that the higher temperature modification corresponds to a trigonal unit cell (SG, $R\bar{3}m$) with its own structure type. In 1975, Chebotarev *et al.*⁹ reinvestigated this

system and found a second allotropic modification at 400 °C confirming the Ni₃Sn crystal structure for the intermediate phase, suggesting that the trigonal crystal structure reported previously by Larson *et al.*¹⁰ actually corresponds to the lowest temperature modification below 400 °C.

Low temperature specific heat measurements of the hexagonal PuGa₃ (DO19 structure) phase revealed a rather large γ value of 225 mJ/mol K².¹¹ However, no magnetic measurements have been reported yet on these binary phases. To shed more light on the nature of the Pu $5f$ electrons in δ -Pu and also in the PuTGa₅ compounds, we have carried out detailed investigations of the thermodynamic, magnetic, and transport properties of the two allotropic phases obtained for PuGa₃.

II. EXPERIMENT

The polycrystalline ingots were obtained by arc melting stoichiometric amounts of the constituent elements under an atmosphere of high purity argon on a water-cooled copper hearth, using a Ti-Zr alloy as an oxygen/nitrogen getter. Starting materials were used in the form of commercial 3N gallium pieces, and by LANL 3N-plutonium metal. In order to ensure homogeneity, the arc melted buttons were turned over and remelted three times, with total weight losses below 0.5%. The samples were characterized by x-ray powder diffraction data (Cu $K\alpha$ radiation) collected on a Bragg-Brentano Siemens D500 diffractometer using a 2θ step size of 0.02 degrees. The diffraction patterns were analyzed by a Rietveld-type profile refinement method using the FULLPROF program.¹² Single crystal x-ray diffraction data were collected on an Enraf-Nonius CAD-4 four-circle diffractometer using monochromated Mo $K\alpha$ radiation. The data processing was carried out using the Molen package.¹³

The magnetization was obtained from a Quantum Design MPMS-7 SQUID in fields up to 7 T and in the temperature range from 2 K to 300 K, using ≈ 17 mg and ≈ 31 mg polycrystalline samples for the high and low temperature phases, respectively. The specific heat was measured on ≈ 4 mg and ≈ 6 mg stycast-encapsulated¹⁴ polycrystalline samples by the relaxation method on a QD-PPMS-9 system in the temperature range 2–300 K and in magnetic fields up to 9 T. The self-heating effects (≈ 2.2 mW/g in the case of the isotopic composition of the Pu batch used in this study) arising from the radioactive isotopes' decay prevented measurements below 4 K. The ambient pressure electrical resistivity data were measured with an ac four-probe technique in a QD PPMS-9 (up to 9 T) on a ~ 8 – 10 mg polycrystalline sample. The high-pressure electrical resistivity measurements were performed on small crystals of typical dimensions $\sim 500 \times 100 \times 40 \mu\text{m}^3$, extracted from polycrystalline ingots. The resistance under pressure was measured by a dc four-probe technique with typical applied current of 1 mA. The sample and a thin foil of lead used as a manometer¹⁵ were mounted in a pyrophyllite gasket and pressurized using steatite as pressure transmitter. The low sample masses ($m < 100 \mu\text{g}$) allowed measurements down to 1.5 K for all pressure points, and down to 0.4 K at the maximum pressure achieved (7.0 GPa) for the trigonal structure.

III. RESULTS

A. Crystal chemistry

The x-ray powder patterns of both the as-cast and the water-quenched from 1020 °C samples of PuGa₃, were successfully indexed using the trigonal unit cell reported in the literature.¹⁰ In agreement with both reported binary phase diagrams,^{8,9} the x-ray powder patterns of annealed sample at 800 °C were refined in the hexagonal Ni₃Sn structure type (S.G., $P6_3/mmc$). The x-ray crystallographic data of the crystal structure determinations are summarized in Tables I and II, with the main interatomic distances.

Finally, the second allotropic transformation reported by Chebotarev *et al.*⁹ could not be confirmed in the present study. Even after 2 months annealing at 380 °C of the 800 °C annealed sample, the XRD powder pattern revealed no other diffraction lines than those arising from the hexagonal structure. This result reveals either very slow kinetics of this transformation, or an erroneous interpretation of Chebotarev experiments, who observed this transformation by heating the fast quenched sample at 400 °C. It may be worth mentioning that whatever the heat treatment performed on PuGa₃, the cubic AuCu₃-type structure adopted by CeIn₃ and UGa₃ could not be obtained in the present experiment.

In the following, the high temperature phase crystallizing in the $R\bar{3}m$ space group will be called the “trigonal phase,” and the low temperature phase crystallizing in the $P6_3/mmc$ space group (DO19 phase, or Ni₃Sn structure type) will be called the “hexagonal phase.”

B. Magnetization

For the trigonal phase, the magnetization curve displays a ferromagnetic transition at $T_C \approx 20$ K (Fig. 1). There is little

difference between the zero-field-cooled and field-cooled curves, even at relatively low magnetic fields, indicating that little energy is required to realign the magnetic domains. Figure 2 clearly shows that the magnetization is already close to saturation ($\mu_{\text{sat}} \approx 0.21 \mu_B$) for fields as low as $\mu_0 H = 0.25$ T. From the hysteresis loop, a weak coercive field $\mu_0 H_c \approx -0.08$ T is inferred. In the paramagnetic state, as shown in the inset of Fig. 1, the susceptibility obeys a modified Curie-Weiss law. A fit of the data yields a positive paramagnetic Curie temperature $\theta_p \approx 15.6$ K, close to the ordering temperature as expected for a ferromagnet, and an effective moment $\mu_{\text{eff}} \approx 0.77 \mu_B$, close to the value expected for Pu³⁺ (configuration $5f^5$) in the Russel-Saunders coupling ($\mu_{\text{eff}} = 0.84 \mu_B$). The term $\chi_0 \approx 175 \times 10^{-6}$ emu/mole is relatively modest, suggesting a limited hybridization of the $5f$ orbitals.

Magnetization measurements of the hexagonal phase, displayed in Figs. 3 and 4, show different behavior. The magnetization data versus temperature (Fig. 3) show first an antiferromagnetic-like transition at 24 K. Upon increasing the applied magnetic field (see inset), the AF transition progressively broadens, whereas a metamagnetic transition slowly appears at low temperature above 6 T and shifts to higher temperature with increasing field. The magnetization versus applied field curve (Fig. 4) is linear and reversible below 6 T at 4.2 K, which confirms the AF like nature of the transition at 24 K. Above 6 T, the metamagnetic transition is clearly observed but does not reach saturation. At 5 K and 7 K, the metamagnetic transition is still observed, at higher magnetic fields, whereas at 10 K it is no longer visible below 7 T. On the other hand, as shown in the inset of Fig. 4, the metamagnetic transition is again visible at 20 K and 22 K. In the paramagnetic state, the susceptibility obeys a modified Curie-Weiss law. The paramagnetic Curie temperature $\theta_p \approx 11.3$ K is positive but lower than that observed for the trigonal modification. The effective moment $\mu_{\text{eff}} \approx 0.79 \mu_B$ is similar and corresponds to the value expected for Pu³⁺. However, the value $\chi_0 \approx 442 \times 10^{-6}$ emu/mole, is significantly higher and suggests a higher hybridization of the $5f$ orbitals in the hexagonal phase than in the trigonal phase. The tentative magnetic phase diagram, represented in Fig. 5, summarizes the results obtained from the magnetization data (full circles).

C. Specific heat

The specific heat $C(T)$ of both structural modifications of PuGa₃ are displayed in Fig. 6.

Trigonal phase: The magnetic phase transition is reflected in a well-pronounced anomaly around $T_C = 20$ K. The transition temperature remains almost unchanged in magnetic fields up to 9 T. The magnetic entropy shifts clearly towards higher temperatures, indicating ferromagnetic order, in agreement with the magnetization data. The γ coefficient of the electronic specific heat derived from the C/T plot at low temperatures, gives a value of $\gamma = (100 \pm 10)$ mJ/mol K² (see inset in Fig. 6).

Hexagonal phase: The onset of antiferromagnetic order at $T_N = 24$ K is confirmed by a clear peak, barely affected by

TABLE I. X-ray crystallographic data of the as-cast PuGa₃ sample, atomic parameters, and interatomic distances.

Method of refinement	Single crystal (Molen)			Powder (Fullprof)		
Space group				<i>R-3m</i> , No. 166		
Lattice parameters	$a=6.180(1)$ Å			$a=6.1911(2)$ Å		
	$c=28.035(5)$ Å			$c=28.089(1)$ Å		
	$V=927.2(5)$ Å ³			$V=932.45(6)$ Å ³		
	$d_{\text{calc}}=9.63$ g cm ⁻³			$d_{\text{calc}}=9.58$ g cm ⁻³		
	$Z=12$			$Z=12$		
	$M=448.2$ g			$M=448.2$ g		
Scan range	$2^\circ < \theta < 30^\circ$			$20^\circ < 2\theta < 110^\circ$		
Wavelength (Å)	Mo <i>K</i> α1			Cu <i>K</i> α		
Reflection used in the refinement	311($I > 3\sigma$)			373/2		
Secondary extinction coefficient	$g=7.7 \times 10^{-7}$					
	corr. = $1/(1+gI_c)$					
Reliability factors	$R_{(E)}$	0.044		R_B	0.080	
	R_W	0.066		R_f	0.054	
	GOF	1.944		R_p	0.124	
				R_{wp}	0.161	
Atom parameters from single crystal refinement						
	Atom	Site	x	y	z	τ_{occ}
	Pu(1)	6 <i>c</i>	0.0	0.0	0.1296(1)	1
	Pu(2)	6 <i>c</i>	0.0	0.0	0.2879(1)	1
	Ga(1)	18 <i>h</i>	0.4792(2)	- x	0.1243(1)	1
	Ga(2)	18 <i>h</i>	0.5007(2)	- x	0.2913(1)	1
Interatomic distances (in Å)						
	Central atom, Pu(1)			Central atom, Pu(2)		
	Ligand atom	Distance		Ligand atom	Distance	
	3Ga(1)	3.0204		3Ga(1)	2.9760	
	3Ga(2)	3.0314		3Ga(2)	3.0513	
	6Ga(1)	3.1093		6Ga(2)	3.0963	
	Pu(1)	4.1295		3Pu(2)	4.2914	

magnetic fields up to 9 T, with a slight shift of magnetic entropy to lower temperatures. The extrapolated γ coefficient from data below 10 K (see inset in Fig. 6) amounts to $\gamma=(205 \pm 10)$ mJ/mol K², in agreement with the value reported in the literature [$\gamma=(225 \pm 20)$ mJ/mol K² (Ref. 10)].

D. Electrical resistivity

Trigonal phase: At ambient pressure, the resistivity shows a plateau at high temperature, followed by a sharp decrease below $T_C \approx 20$ K (Fig. 7). In agreement with magnetization and specific heat data, no field dependency of the resistivity was observed for the trigonal phase (not shown). Applying pressure, the residual resistivity ratio [$RRR=R(300\text{ K})/R(4.2\text{ K}) \sim 1.5$ to 2] are similar to that observed on the bulk sample at ambient pressure, confirming the homogeneity of the samples (Fig. 8). A change of regime appears around 75 K but is not related to any magnetic struc-

ture change in the material. The ferromagnetic transition can still be observed around 21 K for small applied pressures, but the resistivity decrease, already at 0.1 GPa, is much more progressive and distributed over the whole temperature range than at ambient pressure. Indeed, the almost temperature-independent behavior (plateau) in the paramagnetic domain observed for the bulks (ambient pressure) is replaced by a more pronounced “s-shape” curvature. This suggests that this material may display strong anisotropy. The Curie temperature slightly increases with pressure at a rate of +0.45 K/GPa (see inset of Fig. 8). Above 4 GPa, the Curie temperature can no longer be determined.

Hexagonal phase: At ambient pressure, the curve is similar to the trigonal phase, with $R(300\text{ K})/R(4.2\text{ K}) \sim 1.6$, but the change of slope at the transition is more progressive and a small kink is observed at $T_N \approx 24$ K (Fig. 9). The metamagnetic transition is clearly evidenced by magnetoresistance curves (inset of Fig. 9) recorded at different temperatures

TABLE II. X-ray crystallographic data of the 800 °C annealed PuGa₃ sample, atomic parameters, and interatomic distances.

Method of refinement		Powder (Fullprof)				
Space group		<i>P</i> 6 ₃ / <i>mmc</i> , No. 194, DO19				
Lattice parameters		<i>a</i> =6.3148(2) Å <i>c</i> =4.5239(1) Å <i>V</i> =156.23(1) Å ³ <i>d</i> _{calc} =9.53 g cm ⁻³ <i>Z</i> =2 <i>M</i> =448.2 g				
Scan range		20 < 2θ < 140				
Reflection used in the refinement		152/2				
Reliability factors		<i>R</i> _B	0.073			
		<i>R</i> _f	0.051			
		<i>R</i> _p	0.090			
		<i>R</i> _{wp}	0.116			
Atom parameters						
Atom	Site	<i>x</i>	<i>y</i>	<i>z</i>	<i>τ</i> _{occ}	
Pu	2 <i>c</i>	1/3	2/3	1/4	1	
Ga	6 <i>h</i>	0.8524(1)	- <i>x</i>	1/4	1	
Interatomic distances (in Å)						
		Central atom, Pu				
Ligand atom	Distance					
6Ga	2.8948					
6Ga	3.1482					
2Pu	4.2797					

which allow one to confirm and complete the magnetic phase diagram (Fig. 5). It should also be mentioned that the 2 K curve (inset of Fig. 9) exhibits hysteresis arising from the competition between the antiferromagnetic and ferromagnetic exchange interactions in this material.

Under pressure, at 2.5 GPa, the resistivity curve is still very similar to ambient pressure, with a lowest RRR (Fig. 10). Then, for higher pressures, dramatic changes are observed. A decrease of the resistance with pressure is observed with a drastic increase of the RRR ratio from 1.3 at ambient pressure up to 25 at the highest pressure achieved (6.7 GPa). The shape of the curve evolves to a metallic behavior in the temperature range 300 K–20 K. Below 20 K, a T^3 behavior is observed in the high pressure domain ($p > 4$ GPa). The Néel temperature decreases rapidly with pressure at -2 K/GPa (inset of Fig. 10). At pressure higher than 4 GPa, we no longer observe any anomaly, and PuGa₃ shows the metallic aspect in all the temperature range.

IV. DISCUSSION

The discovery of unconventional *d*-wave superconductivity induced by AF spin fluctuations in the CeTIn₅ family^{4,5}

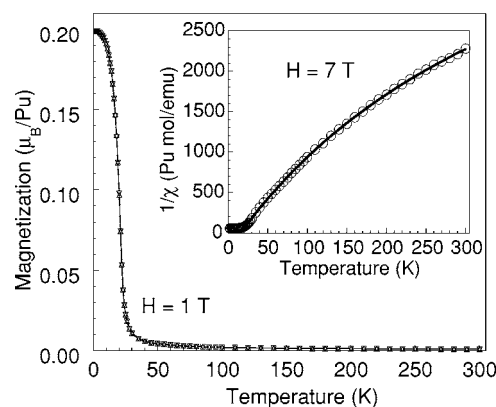


FIG. 1. Zero-field cooled (triangle down) and field-cooled (triangle up) magnetization of the trigonal PuGa₃ versus temperature at $H=1$ T and inverse susceptibility at $H=7$ T (circles, in inset) fitted by a modified Curie-Weiss law (line).

and the cubic binary system CeIn₃ (Ref. 6) emphasizes the dominant role of crystal and magnetic dimensionality in the establishment of magnetically mediated superconductivity.⁷ In the Pu-Ga system, the cubic structure was not observed in the present study, but the two PuGa₃ crystal structures described above display strong similarities with the cubic AuCu₃ type, considering in particular the nearest-neighbor environment of the plutonium sites. The *An*-ligand nearest neighbor interaction seems to be crucial in these systems, as the interactinide distances exceed the Hill limit and no direct *f-f* overlap is expected. The uranium binary phase, UGa₃ (AuCu₃ type),¹⁶ where the U-Ga distances are equal to 2.99 Å at ambient pressure, is considered as a pure itinerant *5f* antiferromagnet system with strong hybridization between the U-*5f* and Ga-*4p* states.¹⁷ In contrast, the neptunium counterpart NpGa₃ (AuCu₃ type, Np-Ga distance 3.01 Å), shows AF/FM behavior,¹⁸ and a model of localized magnet with only slight *5f* hybridization is proposed.¹⁹ Table III shows that the Pu-Ga interatomic distances of the PuGa₃ phases are 3.02 Å and 2.89 Å for the trigonal and the hexagonal phases, respectively. This difference would infer stronger *5f* hybridization in the latter. Indeed, the physical measurements also suggest stronger *5f* delocalization in the hexagonal phase of PuGa₃ that displays higher values of χ_0 and γ values than the trigonal phase. The γ values in both

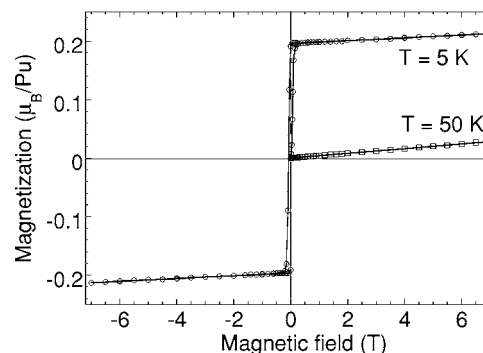


FIG. 2. Magnetization of the trigonal PuGa₃ versus magnetic field at 5 K and 50 K.

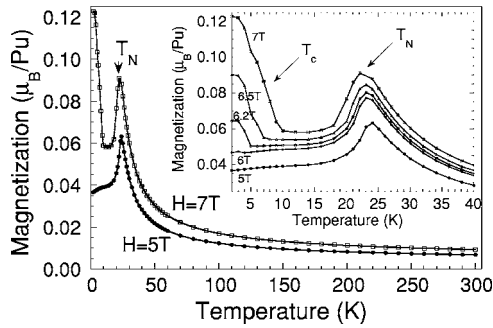


FIG. 3. Magnetization versus temperature under an applied field of 5 T and 7 T of the hexagonal PuGa₃. The inset is a zoom displaying a more detailed measurement under different applied field.

phases of PuGa₃ (100 and 225 mJ/mol K²) are considerably higher than in UGa₃ where a γ value of 52 mJ/mol K² was reported.²⁰ This suggests a rather delocalized character of the 5*f* electrons in the PuGa₃ systems. Unfortunately, no γ value is available for NpGa₃, which prevents a complete comparison. The γ values obtained in PuGa₃ are also significantly higher than that found in PuCoGa₅ ($\gamma=77$ mJ/mol K²),² indicating a high degree of sensitivity of the electronic structure with the Pu-Ga interatomic distances. Finally, it should be mentioned that the PuGa₃ neighboring phase PuGa₂ (Ref. 21) adopts the hexagonal AlB₂-type structure, exhibits AF ordering below $T_N=75$ K, and shows some hints for partial 5*f* localization, similarly to its uranium counterpart UGa₂. Although the Pu environment is different in PuGa₂, it has in common with PuGa₃ to be surrounded by 12 Ga atoms, with a larger interatomic distance (3.2 Å), and specific heat measurements showed small γ value of 12 mJ/mol K².

The hexagonal structure is adopted by a large group of related intermetallic compounds with famous representatives in the heavy fermion family like UPt₃ ($\gamma=450$ mJ/mol K²) (Ref. 22) and CeAl₃ ($\gamma=1600$ mJ/mol K²).²³ The γ coefficient of the electronic specific heat is related to the density of states at the Fermi level and the effective mass of the electrons. Assuming a spherical Fermi surface, one can estimate the Fermi wave vector

$$k_F = (3\pi^2 Z/\Omega)^{1/3}$$

with Ω the volume cell, and the effective mass

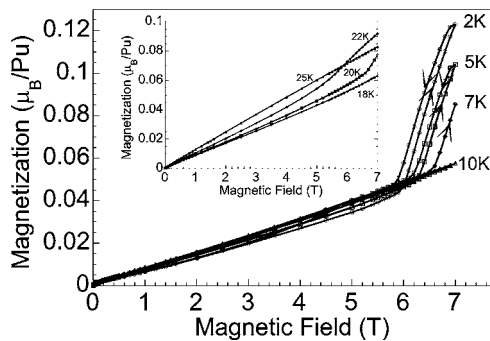


FIG. 4. Magnetization versus field at different temperatures of the hexagonal PuGa₃. The metamagnetic transition is clearly seen at 2 K, then when increasing temperature it disappears and the inset shows its reappearance at 20 and 22 K.

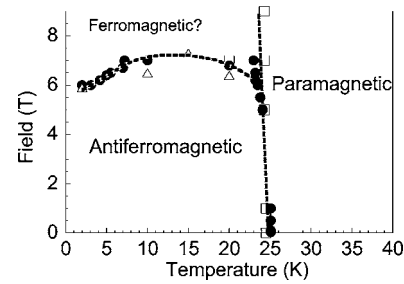


FIG. 5. Magnetic phase diagram of hexagonal PuGa₃ (the full circles display results deduced from magnetization measurements, the triangles are from the electrical resistivity, and the squares from the specific heat).

$$m^* = \hbar^2 k_F^2 \gamma / \pi^2 (Z/\Omega) k_B^2,$$

which leads to an effective mass of 32 and 65 m_0 (electron mass) for the trigonal and the hexagonal PuGa₃ structures, respectively.

The large spatial extension of the 5*f* wave function (compared to the 4*f* one) implies that hybridization plays an important role in the determination of the ground state properties of an actinide-based compound. In such systems, the weakening and destruction of magnetic order are driven by the transition from local to itinerant (bandlike) state rather than by the Kondo effect. The changes of magnetic properties induced by pressure give valuable information about the mechanisms underlying the delocalization of these electrons. Thus, according to Sheng and Cooper,²⁴ the decrease of the interatomic distances caused by pressure induces the 5*f* wave functions to diffuse more outside the core region. This in turn increases the hybridization between the 5*f* electrons and the band states of the compound, which enhances the exchange-coupling J and may thus strengthen magnetic order to a certain extent. In the weakly correlated ferromagnet UTe,²⁵ T_c first increases under pressure before decreasing. Pressure measurements reveal a fast collapse of AF magnetic order in the itinerant antiferromagnet UGa₃ (Refs. 26 and 27) while magnetism of the quasilocalized NpGa₃ is reinforced with an increase of the ordering temperature under pressure.¹⁹ The trigonal phase of PuGa₃ can be compared to NpGa₃, while the hexagonal phase would rather compare to UGa₃. Indeed,

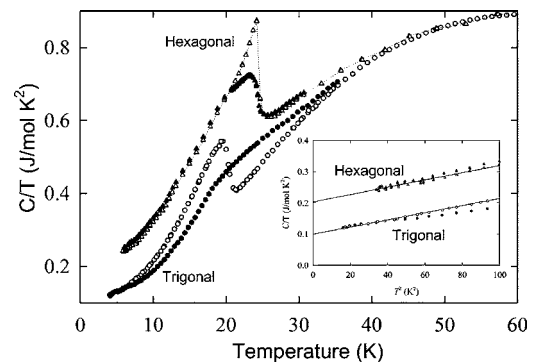


FIG. 6. Specific heat of both PuGa₃ structural modifications; inset shows the low temperature part used to determine the γ parameter.

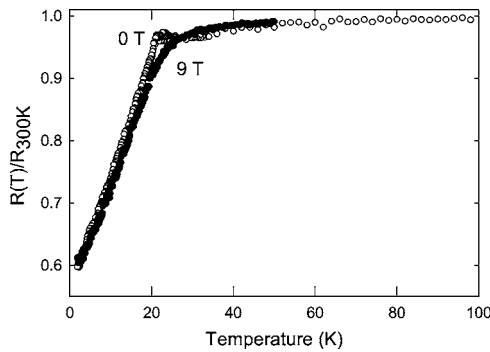


FIG. 7. Ambient pressure magnetoresistivity measurement of the trigonal PuGa_3 .

in the trigonal phase of PuGa_3 , resistivity measurements clearly show a linear increase with pressure of the ferromagnetic interactions, whereas in the more delocalized hexagonal phase pressure weakens magnetic order.

It is worth emphasizing that magnetic and superconducting transition temperatures are one order of magnitude higher in the $An\text{TGa}_5$ compounds^{2,3,7} compared to the CeTIn_5 systems.^{5,6} The analogy of PuGa_3 with CeIn_3 ,⁶ suggests that we should observe a collapse of magnetism under pressure toward a quantum critical point (QCP).⁶ However, in the trigonal structure, we observe a reinforcement of the ferromagnetic interactions with pressure and the weak dependency of the RRR with pressure indicates that we are far away from a QCP. On the contrary, in the hexagonal phase, the drastic change of the electrical resistivity curve displayed in Fig. 10 and the collapse of magnetism around 3–4 GPa are hints of approaching a QCP. However, precise analysis of the low temperature resistivity ($\sim T^3$) does not fit with other features of a QCP like the appearance of a Fermi liquid regime ($\sim T^2$).²⁸ Moreover, the metallic regime at high pressure is clearly different from magnetic fluctuations mediating superconductivity like those occurring in CeIn_3 (Ref. 6) or CePd_2Si_2 (Refs. 28 and 29) and we do not observe any superconducting signal down to 1.5 K. We conclude that, despite very favorable ground state properties showing heavy fermion features with high γ and effective mass with a collapse of AF ordering with pressure, magnetic fluctuations are probably too strong to mediate superconductivity in the pressurized hexagonal structure.

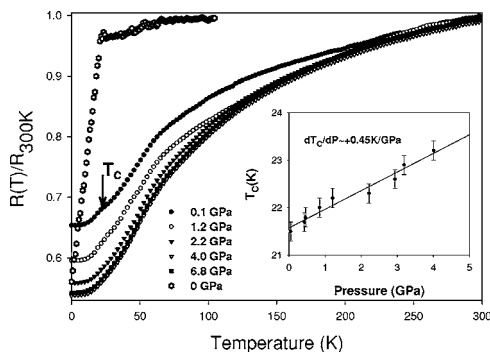


FIG. 8. Ambient pressure magnetoresistivity measurement of the hexagonal PuGa_3 . The inset shows the field dependency at various temperatures.

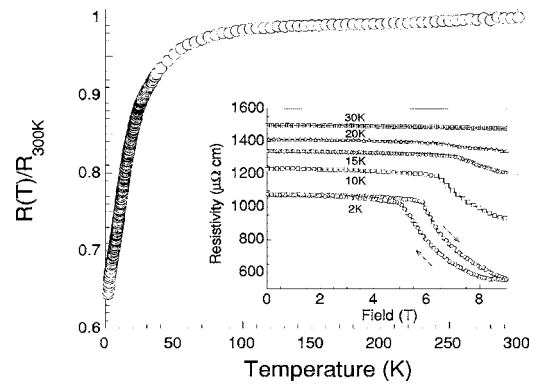


FIG. 9. Normalized curves $R(T)/R_{300\text{ K}}$ of the trigonal modification of PuGa_3 at several pressures. Inset shows the evolution of the ferromagnetic ordering temperature with pressure.

Both PuGa_3 phases show similar effective magnetic moments, around $0.78\mu_B/\text{Pu}$ atom, consistent with the Pu^{3+} charge state. This result is somewhat surprising, taking into account the differences between both phases discussed above, but can be related to NpPd_3 (Ref. 30) for which similar behavior was observed with the high temperature phase crystallizing in the AuCu_3 type and the low temperature modification showing the hexagonal DO_{24} type.

As already mentioned, from the structural point of view these two phases are related to the PuTGa_5 ternary systems, where actinide atoms are located in the octahedral site occupied by Ga in PuGa_3 . In fact T atoms can be considered here as perturbing elements since they do not directly bond with Pu, and that in the case of PuCoGa_5 , the Co 3d states are almost not at the Fermi levels. In PuCoGa_5 , the Pu-Ga interatomic distance 2.99 Å is intermediate between those observed for both PuGa_3 phases. Band structure calculations using LSDA (Ref. 31) indicates stronger hybridization between Pu-5f and Ga-4p states in the vicinity of the Fermi level. Moving from $An\text{Ga}_3$ to $An\text{TGa}_5$ systems seems to result in more delocalized 5f electrons. The itinerant antiferromagnet UGa_3 is to be compared to the mixed valence compound UCoGa_5 ,³² and the quasilocalized NpGa_3 compared to the moderately delocalized NpCoGa_5 .³³ This trend is compatible with a moderately delocalized 5f character of the magnetically ordered trigonal and hexagonal phases of

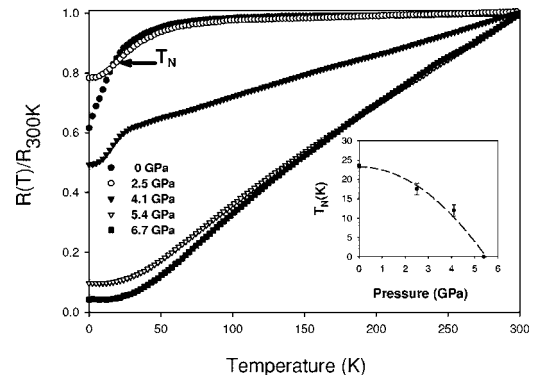


FIG. 10. Normalized curves $R(T)/R_{4.2\text{ K}}$ of the hexagonal PuGa_3 at several pressures. Inset shows the decrease of the AF magnetic ordering with pressure.

TABLE III. Magnetic properties of $AnGa_3$ compounds ($An=U, Np, Pu$).

Compounds	An polyhedral	An -Ga distance	Density	μ_{eff}	μ_0 (μ_B)	T_N/T_C (K)	χ_0 (emu/mol)	θ_p (K)	λ (mJ/mol K ²)
UGa ₃ ($Pm-3m$)	Octahedral	2.99	9.69		0.8	$T_N=67$ K			52
NpGa ₃ ($Pm-3m$)	Octahedral	3.00	9.66		1.5	$T_N=65$ K			
PuGa ₃ ($R-3m$)	$\frac{1}{2}$ Octahedral, $\frac{1}{2}$ trigonal	3.02	9.60	0.77	0.21	$T_C=20$ K	175	15.6	100(10)
PuGa ₃ ($P6_3/mcm$)	Trigonal	2.89	9.53	0.79		$T_N=24$ K	442	11.3	205(10)

PuGa₃ compared to a more delocalized $5f$ character of the paramagnetic superconductor PuCoGa₅.

V. CONCLUSION

Contrary to its uranium and neptunium counterparts, PuGa₃ does not crystallize with the cubic AuCu₃-type structure. Depending on the annealing temperature, two distinct structures, trigonal and hexagonal, both closely related to the AuCu₃ type, are observed. Despite some strong analogies with CeIn₃, in particular the hexagonal phase of PuGa₃ that exhibits heavy fermion features and a collapse of antiferromagnetism under pressure, no superconductivity is observed in both phases of PuGa₃ down to 1.5 K and up to 7 GPa. Instead, these two allotropic phases order ferromagnetically at $T_C=21$ K (trigonal) and antiferromagnetically at $T_N=24$ K (hexagonal) displaying high γ values (100 and 225 mJ/mol K², respectively) which classify them as moderate heavy fermions. The pressure dependence of the magnetic interactions, showing a linear decrease of the antiferro-

magnetic interactions in one case and the reinforcement of the ferromagnetic interactions in the other case, is a signature of delocalized systems, and compressibility study should provide useful information to confirm this behavior.

ACKNOWLEDGMENTS

We are grateful to G. H. Lander and P. M. Oppeneer for fruitful discussions. Work of one of the authors (P.J.) is a part of the research program MSM113200002 financed by the Ministry of Education of the Czech Republic. Work in Florida was performed under the auspices of the US Department of Energy Contract No. DE-FG05-86ER45268. One of the authors (E.D.B.) acknowledges financial support from the Seaborg Postdoctoral Fellowship Program. The high purity Pu metals required for the fabrication of the compounds was made available through a loan agreement between Lawrence Livermore National Laboratory and ITU, in the frame of a collaboration involving LLNL, Los Alamos National Laboratory and the US Department of Energy.

¹For review see, e.g., S. S. Hecker, D. R. Harbur, and T. G. Zocco, Prog. Mater. Sci. **49**, 429 (2004), and references therein.

²J. L. Sarrao, L. A. Morales, J. D. Thompson, B. L. Scott, G. R. Stewart, F. Wastin, J. Rebizant, P. Boulet, E. Colineau, and G. H. Lander, Nature (London) **420**, 317 (2002).

³F. Wastin, P. Boulet, J. Rebizant, E. Colineau, and G. H. Lander, J. Phys.: Condens. Matter **15**, 2279 (2003).

⁴C. Petrovic, R. Movshovich, M. Jaime, P. G. Pagliuso, M. F. Hundley, J. L. Sarrao, Z. Fisk, and J. D. Thompson, Europhys. Lett. **53**, 354 (2001).

⁵H. Hegger, C. Petrovic, E. G. Moshopoulou, M. F. Hundley, J. L. Sarrao, Z. Fisk, and J. D. Thompson, Phys. Rev. Lett. **84**, 4986 (2000).

⁶N. D. Mathur, F. M. Grosche, S. R. Julian, I. R. Walker, D. M. Freye, R. K. W. Haselwimmer, and G. G. Lonzarich, Nature (London) **394**, 39 (1998).

⁷E. D. Bauer, J. D. Thompson, J. L. Sarrao, L. A. Morales, F. Wastin, J. Rebizant, J. C. Griveau, P. Javorsky, P. Boulet, E. Colineau, G. H. Lander, and G. R. Stewart, Phys. Rev. Lett. **93**,

147005 (2004).

⁸F. H. Ellinger, C. C. Land, and V. O. Struebing, J. Nucl. Mater. **12**, 226 (1964).

⁹N. T. Cheboratev, E. S. Smotriskaya, M. A. Andrianov, and O. E. Kostyuk, "Plutonium and others actinides," Proceedings of the 5th International Conference, Baden Baden, 1975 (1976), p. 37.

¹⁰A. C. Larson, D. T. Cromer, and R. B. Roof, Acta Crystallogr. **18**, 294 (1965).

¹¹G. R. Stewart, B. Andraka, and R. G. Haire, J. Alloys Compd. **213/214**, 111 (1994).

¹²J. Rodriguez-Carvajal, Physica B **192**, 55 (1993).

¹³C. K. Fair, *Molen Users Manual—An Interactive Intelligent System for Crystal Structure Analysis* (Delft, Netherlands, 1989).

¹⁴P. Javorský, E. Colineau, J. Rebizant, P. Boulet, G. Stewart, and F. Wastin, J. Nucl. Mater. (to be published).

¹⁵B. Bireckhoven and J. Wittig, J. Phys. E **21**, 841 (1988).

¹⁶D. Kaczorowski, R. Troc, D. Badurski, A. Böhm, L. Shlyk, and F. Steglich, Phys. Rev. B **48**, 16425 (1993).

¹⁷D. Mannix, A. Stunault, N. Bernhoeft, L. Paolasini, G. H. Lander,

- C. Vettier, F. de Bergevin, D. Kaczorowski, and A. Czopnik, *Phys. Rev. Lett.* **86**, 4128 (2001).
- ¹⁸E. Colineau, F. Bourdarot, P. Bulet, J. P. Sanchez, and J. Larroque, *Physica B* **230**, 773 (1997).
- ¹⁹S. Zwirner, V. Ichas, D. Braithwaite, J. C. Waerenborgh, S. Heathman, W. Potzel, G. M. Kalvius, J. C. Spirlet, and J. Rebizant, *Phys. Rev. B* **54**, 12283 (1996).
- ²⁰M. H. van Maaren, H. J. van Daal, K. H. J. Buschow, and C. J. Schinkel, *Solid State Commun.* **14**, 145 (1974).
- ²¹P. Boulet, E. Colineau, P. Javorský, F. Wastin, and J. Rebizant, *J. Alloys Compd.* **394**, 93 (2005).
- ²²A. De Visser, J. J. M. Franse, A. Menovsky, and T. T. M. Palstra, *Physica A* **127**, 442 (1984).
- ²³K. Andres, J. E. Graebner, and H. R. Ott, *Phys. Rev. Lett.* **35**, 1779 (1975).
- ²⁴Q. G. Sheng and B. R. Cooper, *J. Appl. Phys.* **75**, 7035 (1994).
- ²⁵P. Link, U. Benedict, J. Wittig, and H. Wühl, *J. Phys.: Condens. Matter* **4**, 5585 (1992).
- ²⁶M. Nakamura, Y. Koike, N. Metoki, K. Kakurai, Y. Haga, G. H. Lander, D. Aoki, and Y. Onuki, *J. Phys. Chem. Solids* **63**, 1193 (2002).
- ²⁷G. E. Grechnev, A. S. Panfilov, I. V. Svechkarev, A. Delin, B. Johansson, J. M. Wills, and O. Eriksson, *J. Magn. Magn. Mater.* **192**, 137 (1999).
- ²⁸F. M. Grosche, I. R. Walker, S. R. Julian, N. D. Mathur, D. M. Freye, M. J. Steiner, and G. G. Lonzarich, *J. Phys.: Condens. Matter* **13**, 2845 (2001).
- ²⁹I. Sheikin, E. Steep, D. Braithwaite, J.-P. Brison, S. Raymond, D. Jaccard, and J. Flouquet, *Low Temp. Phys.* **122**, 591 (2001).
- ³⁰W. J. Nellis, A. R. Harvey, G. H. Lander, B. D. Dunlap, M. B. Brodsky, M. H. Mueller, J. F. Reddy, and G. R. Davidson, *Phys. Rev. B* **9**, 1041 (1974).
- ³¹I. Opahle and P. M. Oppeneer, *Phys. Rev. Lett.* **90**, 157001 (2003).
- ³²R. Troc, Z. Bukowski, C. Sulkowski, H. Misiorek, J. A. Morkowski, A. Szajek, and G. Chelkowska, *Phys. Rev. B* **70**, 184443 (2004).
- ³³E. Colineau, P. Javorský, P. Boulet, F. Wastin, J. C. Griveau, J. Rebizant, J. P. Sanchez, and G. R. Stewart, *Phys. Rev. B* **69**, 184411 (2004).